Available online at www.sciencedirect.com
SCIENCE DIRECT®
Polymer 44 (2003) 4705–4713
polymer
www.elsevier.com/locate/polymer

Microstructure and properties of polyimide/poly(vinylsilsesquioxane) hybrid composite films

Mohammad A. Wahab, Il Kim, Chang-Sik Ha*

Department of Polymer Science and Engineering, Pusan National University, Pusan 609-735, South Korea

Received 6 January 2003; received in revised form 25 March 2003; accepted 5 May 2003

Abstract

Polyimide (PI)/poly(vinylsilsesquioxane) (PVSSQ) (PI/PVSSQ) hybrid composite films were prepared from 3,3′,4,4′-biphenyltetracarboxylic dianhydride (BPDA)–4,4′-oxydianiline (ODA) polyamic acid and triethoxyvinylsilane (TEVS or VSSQ) via sol–gel process and thermal imidization. The presence of the PVSSQ showed a remarkable effect on the microstructure and properties of the polyimide based hybrid films. The transparency of the hybrid films decreased with increasing the content of the PVSSQ. The compatibility and interfacial interaction of the hybrid composites were evaluated by scanning electron microscope (SEM) and atomic force microscope (AFM), respectively. The PI/PVSSQ hybrids showed nanocomposite formation when the contents of PVSSQ was less than 20 wt%. It was found that the surface topography was influenced by the composition of the PVSSQ. Incorporating of the PVSSQ increased the thermal stability and T_g of hybrid composites. The dielectric constant of the hybrid composites was reduced by adding PVSSQ up to a certain content, showed a minimum and then found to be increased. The dielectric constant values of the hybrid composites ranged from 2.59 to 3.78. The presence of the PVSSQ also showed significant effects on the mechanical properties of the polyimide films.

Keywords: Low dielectric constant; Polyimide/silica hybrid composites; Silsesquioxane

1. Introduction

Organic–inorganic hybrids have attracted much interest, since they usually combine desirable organic and inorganic characteristics [1]. These hybrid materials are usually produced by sol–gel reaction which consists of two step reaction: hydrolysis of metal alkoxides to produce hydroxyl groups, followed by the polycondensation of the hydroxyl groups and residual alkoxy groups to form a three-dimensional network. In these hybrid composites, polyimides (PIs) have been widely applied as matrix polymers for the advanced applications such as in the aerospace and the microelectronics industries due to their outstanding characteristics such as good chemical and mechanical properties as well as low dielectric constant [2–5]. In addition, silica has been widely used as an inorganic component in hybrid composites to achieve various properties to meet the requirements of different applications [6–19].

Recently, there has been a great deal of interest in polysilsesquioxane (PSSQ) among the chemists, physicists, material scientists, and integration engineers for advanced technology such as low dielectric insulators in microelectronic devices [20,21] and novel reinforcing elements for hybrid composites [22,23]. Since PSSQ with an organic group has low dielectric constant and low moisture absorption compared to silica, it has already been proposed as replacement for silicon dioxide [20]. The silica based PSSQ has been known to possess not only low dielectric constant but also high thermal stability. Although, the polyimide/PSSQ hybrid composites are new type of materials, there are only few studies on the syntheses and their properties [6,11,24–29]. It is evident that the nature of the organic substituents plays an important role in determining the microstructure and properties of the polyimide hybrids containing PSSQ. The control of microstructure, molecular weights, and the nature of remaining functional end groups are important for the mechanical properties of final composites [30]. The sound relationships between structures of the PSSQ and properties of the PIs have not been well established yet. A detailed

* Corresponding author. Tel.: +82-51-510-2407; fax: +82-51-514-4331.
E-mail address: csha@pusan.ac.kr (C.S. Ha).

0032-3861/03/$ - see front matter © 2003 Elsevier Science Ltd. All rights reserved.
doi:10.1016/S0032-3861(03)00429-4

systematic investigation on the microstructure and interaction between PSSQ and PIs are needed. In this paper, therefore, we wish to report the effect of the PSSQ on the microstructure, interfacial interaction, and properties of the polyimide based hybrid films. For this work, poly(vinylsilsesquioxane) (PVSSQ) was investigated as one type of the PSSQ.

2. Experimental

2.1. Materials

3,3′,4,4′-biphenyltetracarboxylicdianhydride (BPDA), 4,4′-oxydianiline(ODA), tetraethoxyorthosilicate (TEOS), triethoxyvinylsilane (TEVS), and anhydrous dimethylacetamide (DMAc), obtained from Aldrich, were used as received.

2.2. Preparation of hybrid films

As shown in Fig. 1, hybrid films were prepared by making polyimide precursor solution in DMAc, then incorporating TEVS or TEOS and mixing to a homogeneous state, followed by adding deionized water; the sol–gel reaction then took place, followed by spin-coating the resulting silica sol/polyimide precursor solution onto a glass substrate, soft-baking the films, and finally imidizing the films thermally. The BPDA–ODA PAA solution was prepared with equimolar ratio of BPDA and ODA in DMAc under nitrogen atmosphere. The reaction was continued for 24 h to make a homogeneous mixture. Different weight percentage of TEVS with stoichiometric amount of water was added into the reaction mixture with stirring for overnight to form homogeneous solution. The solid content of the solution was 13.5 wt%. The reaction mechanisms of the sol–gel process of TEVS (or TEOS) are shown in Fig. 2. The imidization process was carried out at 60 °C for 2 h, 80 °C for 2 h, 200 °C for 1 h and 300 °C for

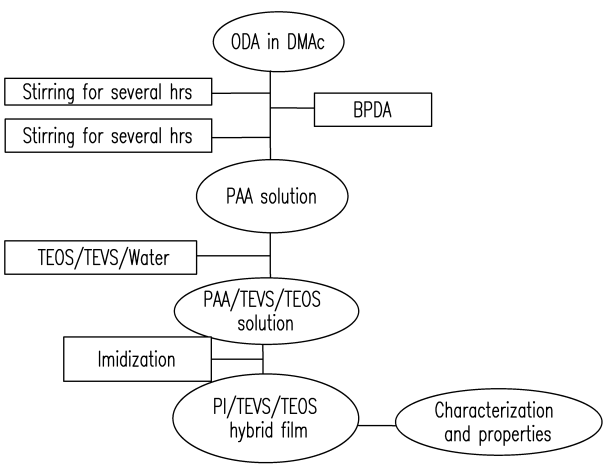

Fig. 1. Preparation of PAA, PAA/TEVS/TEOS and hybrid films.

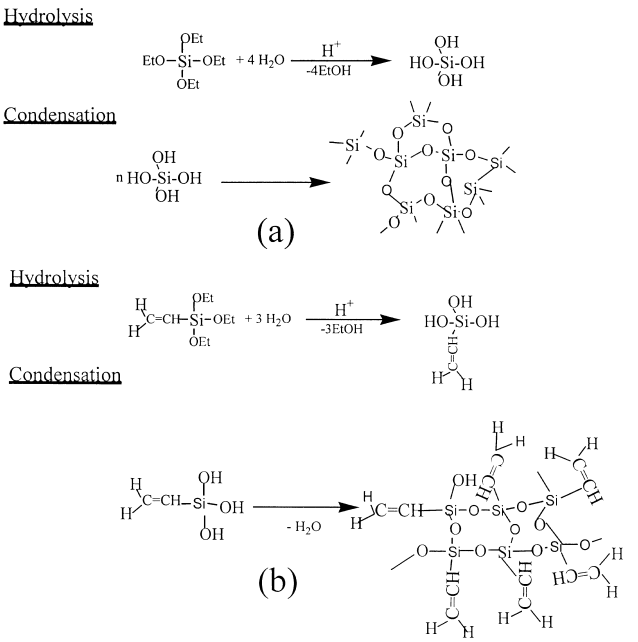

Fig. 2. Sol–gel process of tetraethoxysilane (a) and TEVS (b); hydrolysis and condensation occurs simultaneously.

1 h in a vacuum under nitrogen atmosphere to get hybrid films. The heating rate was 2 °C/min. The chemical structures of BPDA and ODA and their conversion from monomers to polyamic acid (PAA) and BPDA–ODA PI are shown in Fig. 3. PI/TEOS/TEVS hybrid films as well as PI/TEOS hybrid of 30 wt% of TEOS were also prepared by similar procedures as those of PI/TEVS hybrids. Sample codes are summarized in Table 1.

2.3. Measurements and characterization

Fourier Transform Infrared (FTIR) analyses of hybrids were performed with a React IR (React IR™ 1000, Applied System, ASi). Scanning electron microscope (SEM; Hitachi S-4200) and atomic force microscope (AFM;Nanoscope III,® Digital Instruments Co.) were used to investigate the morphology of the hybrid films. Prior to SEM measurements, the fractured surfaces from liquid nitrogen were gold coated. AFM images were taken with 5 × 5 μm scan area from 1 × 1 cm hybrid films. Thermo-gravimetric analyzer (Perkin–Elmer TGA-7) was used to investigate the thermal stability of polyimide and hybrid films. The heating rate was 20 °C/min in nitrogen atmosphere. The transparency of the hybrid films was measured with UV–Visible–Near IR spectrophotometer (CARY 5E, Varian Co.) at 638 nm. The thickness of the films was about 100 nm. Mechanical properties were measured using a UTM machine (Tenius Oisen 1000, Digital Indicator Green PL 9700W). The gauge length was 50 mm and crosshead speed was 2 mm/min. Three samples were averaged. Dynamic mechanical properties were measured using a dynamic mechanical thermal analyzer (DMTA) (Rheometrics Dynamic Analyzer RDA II, Resource Series) with heating rate of 5 °C/min at 1 Hz.

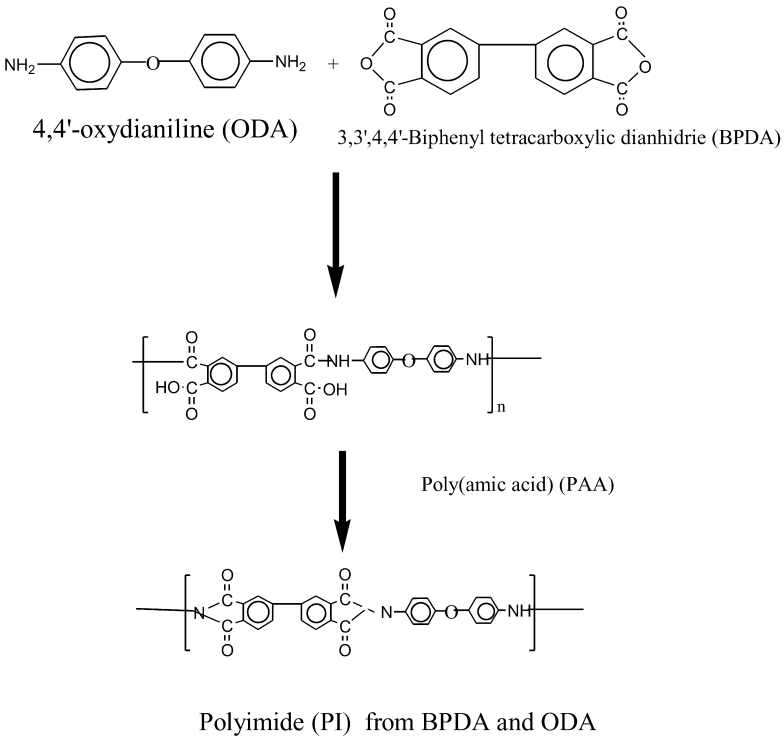

Fig. 3. Conversion from the BPDA-ODA PAA to the BPDA-ODA PI.

The dielectric constant was obtained at 1 MHz with the Impedance-Gain Phase Analyzer (HP4194A) using the formula $K = Cd/A\varepsilon_O$, where C is the observed capacitance, d the film thickness, A the gold area, and ε_O the free permittivity. The thickness of the films was 0.14 ± 0.01 μm.

3. Results and discussion

3.1. General observations

Table 1 summarizes the preparation conditions and the transparency of hybrid composite films. It was observed that the films become opaque when the PVSSQ value ≥20%. It means that silica domain size become larger during imidization process. The transparency of the hybrid films shown in Table 1 indicates that the transparencies of the hybrid films decrease with increasing the content of PVSSQ. The phenomenon comes from the increase of the PVSSQ domain sizes with increasing PVSSQ content, resulting in high scattering. It should be noted, however, that hybrid films containing PVSSQ were more flexible in all compositions compared to the hybrid films containing silica from TEOS, which was already reported by the authors [18].

3.2. FTIR analysis

Fig. 4 shows FTIR spectra of the pure polyimide and hybrid composite films. Upon curing, the characteristic

Table 1
Preparation of PAA, PAA–TEVS/TEOS and hybrid composite films

Sample code	PAA (g)	TEVS (g)	TEOS (g)	PVSSQ or Silica[a] (wt%)	Film state[b]	T[c] (%)
PAA	6.3364				T	–
PI/TEVS5	6.3364	0.3168		5	T	90
PI/TEVS10	6.3364	0.6336		10	T	86
PI/TEVS20	6.3364	1.2672		20	O	82
PI/TEVS30	6.3364	1.9009		30	O	75
PI/TEOS30	6.3364	1.9009		30	O	–
PI/TV25TE75	6.3364	0.4752	1.4256	30	O	–
PI/TV50TE50	6.3364	0.9504	0.9504	30	O	–
PI/TV75TE25	6.3364	1.4256	0.4752	30	O	–

[a] PVSSQ or silica content (wt%) in hybrid composites films was calculated by assuming that sol–gel reaction was completed.
[b] T; Transparent, O; Opaque.
[c] Under visible light at 638 nm, '–' not determined.

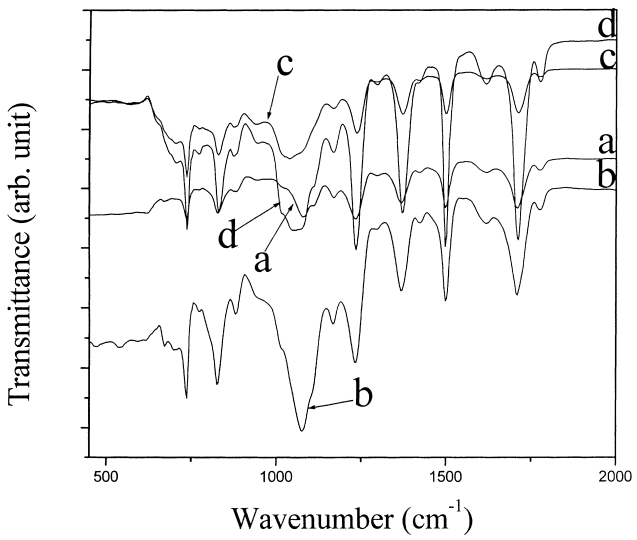

Fig. 4. IR spectra of polyimide and hybrid composite films (a): pure polyimide, (b): PI/TEVS30, (c): PI/TEOS30, and (d): PI/TE25/TV75.

adsorption peaks of imide groups are present near at 1780, 1711, 1368, and 730 cm^{-1} in the hybrid samples as well as PI. Among them, the peaks at 1711 cm^{-1}, representing an imide group, and 1780 cm^{-1}, indicating a cyclic five-membered ring, confirmed imide formation. The bands at 1368 and 730 cm^{-1} are attributed to the C–N–C bond and the imide ring deformation, respectively. The bands at 1502 and 830 cm^{-1} correspond to C_6H_4 and Si–O–Si, respectively. The band at 1173 cm^{-1} is attributed to the C_6H_4 or C_6H_2. The peak at 677 cm^{-1} is assumed due to C–C=O in plane swing vibration. FTIR was also evaluated to verify imidization of the PAA by observing the disappearance of the band at 1650 cm^{-1} and the growth of the imide group at 1711 cm^{-1}. This observation showed a good agreement with the earlier studies [11,17,24,27,31]. The bands at 1626 and 1421 cm^{-1} correspond to the Si–CH=CH_2 group [32]. The $-CH_2-$ wagging vibration of Si–CH=CH_2 at 930 cm^{-1} are also appeared in the hybrid spectra in Fig. 4.

The peak at 884 cm^{-1} corresponds to the Si–OH bond or C_6H_4. The broad band near 1080 cm^{-1}, caused by the presence of the Si–O–Si bond, is indicative of the network formation in the hybrid composites. This band is broader for the PI/TEOS30 hybrid (c) than for PI/TEVS (b) and PI/TE25/TV75 (d) hybrid materials. The narrowing of this band in the latter hybrid materials indicates that the silica environment for PI/TEVS30 and PI/TE25/TV75 hybrid materials is more homogeneous than for the PI/TEOS30 hybrid. However, the intensities of spectra b and d are higher compared to the spectrum c. It means that PI hybrid materials containing PVSSQ showed better homogeneity compared to the PI hybrid containing TEOS, which will be supported by our SEM and AFM images (Figs. 5 and 6). The peak intensities at 1626 and 1421 cm^{-1} are higher for the PI/TEVS30 and the PI/TE25/TV75 hybrids in comparison to those of the PI/TEOS30 hybrid (spectrum c), suggesting the characteristic peak of TEVS. The new absorption peaks at 769 and 801 cm^{-1} might be associated with the inter cross-liking between the polyimide and silica network. The observation of the Si–O–C bond at 978 cm^{-1}, however, indicates the presence of unhydrolized ethoxy substitutents, suggesting incomplete hydrolysis. These features are produced by the presence of TEVS because of its lower functionality ($f = 3$) and the steric hindrance introduced by the vinyl group [11].

3.3. Microstructure of polyimide/PVSSQ or polyimide/TEOS hybrid films

The SEM micrographs of fractured surfaces are shown in Fig. 5. Fig. 5(a)–(c) reveals that the domain size of PVSSQ is less than 50 nm for the polyimide/PVSSQ hybrids of PVSSQ $\leq$20 wt% contents, meaning the nanocomposite formation. Fig. 5 shows the presence of some interconnected silica domains, especially, below 20 wt% of PVSSQ in the continuous polyimide phase. The enhancement of phase compatibility brought by the use of organic PVSSQ may be associated with better interfacial interaction in the PI/PVVSQ hybrid in comparison to that of the PI/TEOS hybrid system. The interaction may include some inter cross-liking between the polyimide and silica network due to the presence of vinyl groups, as already shown in Fig. 4. Moreover, the end hydrogen of PVSSQ as well as the hydrogen of Si–OH may also provide hydrogen bonds with the carbonyl groups in the polyimide matrix, leading to enhance the compatibility of silica with polyimide. Comparing Fig. 5(d) and (e), one can see that the phase morphology is much better for the polyimide hybrid containing PVSSQ than for the polyimide containing TEOS. The micrographs in Fig. 5 showed that the morphologies of both the hybrids containing 30 wt% of PVSSQ and TEOS are quite similar, both revealing the presence of fairly spherical particles dispersed in the polyimide matrix, indicating the formation of microcomposites. On the other hand, for the hybrids containing TEOS/TEVS mixtures, there exist gross phase separation due to the incompatibility between components. The clearer phase separation is observed, as the contents of TEOS are higher. The better compatibility between PVSSQ and polyimide rather than that between silica from TEOS and polyimide may be also expected in the literature [6,27].

The AFM images of the surface topography obtained for the representative composite films with different amount of PVSSQ are shown in Fig. 6. For comparison, AFM images of the PI/TEOS hybrid of 30 wt% of TEOS are also shown. In the 2D images, bright domains are the inorganic particles. It is clearly seen in Fig. 6 that the surface of the PI/PVSSQ hybrids is slightly different from that of the PI/TEOS30 hybrid in terms of roughness. The roughness of the composite films containing 30 wt% of the PVSSQ or TEOS was higher than that of the composite films containing below 30 wt% of PVSSQ, which is related to the phase separation between the PI and PVSSQ or TEOS. The

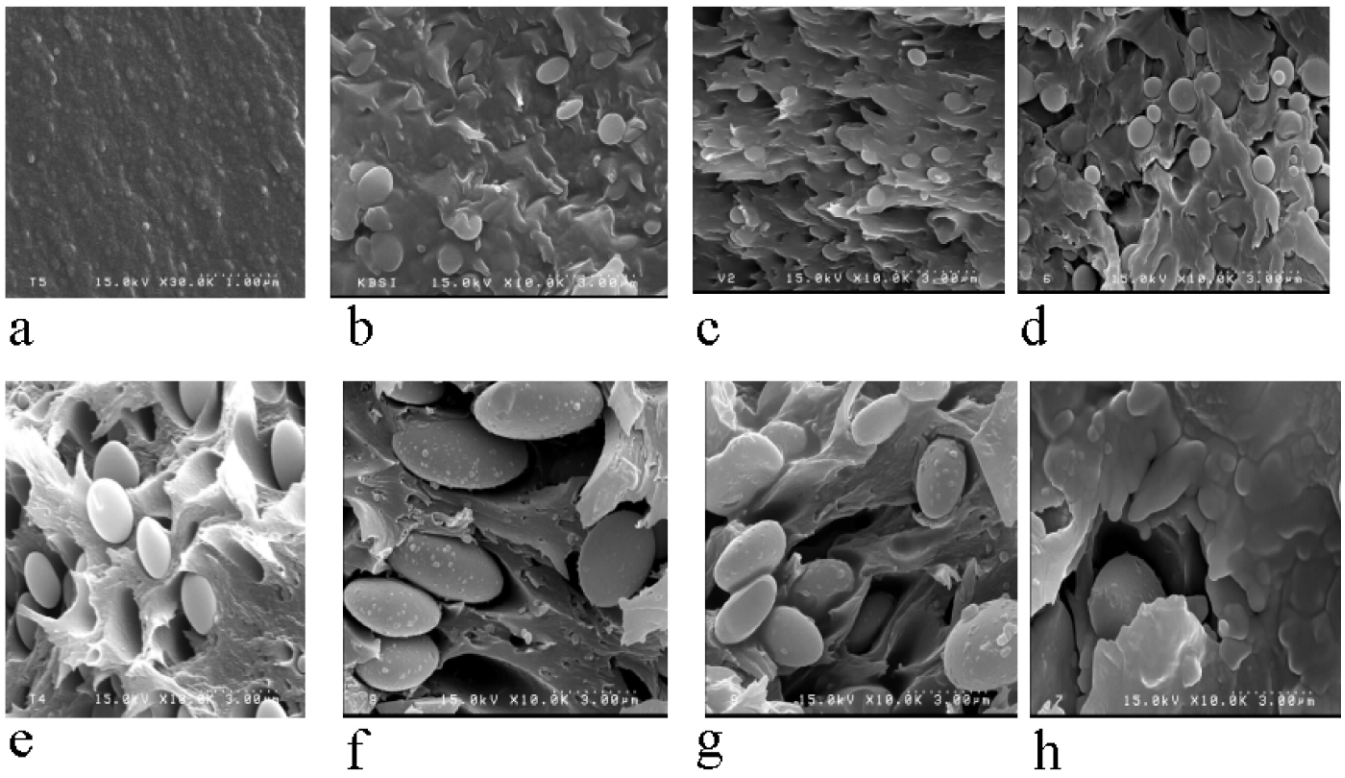

Fig. 5. Fractured surface morphology of hybrid composite films (a): PI/TEVS5, (b): PI/TEVS10, (c): PI/TEVS20, (d): PI/TEVS30 (e): PI/TEOS30, (f): PI/TV25TE75, (g): PI/TV50TE50, and (h): PI/TV75TE25.

PVSSQ is more segregated from the PI phase to form larger domains called 'islands' in the 'sea-island' structure, which may be formed during microphase separation as the contents of PVSSQ is increased. In the surface, these domains are integrated to form large mounds of particle shape with increasing the roughness. The small islands generated from the smaller amounts of the PVSSQ are finely separated to stand up on the surface with a shape of steep valleys, as shown in Fig. 6(a)–(c). This type of morphological difference may be also influenced by the difference in compatibility between the PVSSQ and PI depending on the PVSSQ contents. The central portion of the 2D image was reconstructed as a 3D image to investigate more precisely the hybrid composite film surface. Comparison of Fig. 6(e) and (d) also shows that the PI/PVSSQ hybrid shows better surface morphology than that of the PI/TEOS hybrid at the same silica contents (30 wt%). The 3D images show that inorganic particles seem to be embedded in the film surface. The surface roughness of the hybrid composite films was estimated from the AFM data and plotted against the PVSSQ or TEOS compositions in Fig. 7. However, the surface roughness values of the hybrid composites have been found to be almost indifferent up to 20 wt% of the PVSSQ, then found to be increased with increasing contents of the PVSSQ. Overall inspection of the AFM images suggested that interfacial interaction in the PI/PVSSQ30 hybrid is better compared to the PI/TEOS30 hybrid. These images may demonstrate that a strong bond has been formed between the PVSSQ and the PI matrix in the composites by penetration of the PVSSQ into the polyimide matrix [33].

3.4. Thermo-mechanical properties

Thermo-gravimetric curves of pure polyimide and hybrid composites are shown in Figs. 8 and 9. TGA curves indicate that water or solvent has been successfully removed from the polyimide film and hybrid films because there is no weight loss below 100 °C. It is clearly shown in Fig. 8 that the thermal stability of the PI is increased by incorporation of the PVSSQ in terms of the weight residues above 750 °C. The increase in the weight residues above 750 °C suggests successful incorporation of higher amount silica into the hybrid materials and ultimately increases in thermal stability. The improvements in the thermal stability of hybrid composites mainly come from the strong interaction/chemical bonding between the polyimide and the PVSSQ molecules and the possible penetrated network structure of hybrids [34]. Fig. 9 suggests, however, that the thermal stability of the hybrid increases with increasing TEOS contents in the TEOS/TEVS containing hybrids. It may be assumed that the thermal stability of organic materials can be improved by introducing inorganic components such as silica, on the basis of the fact that these materials have inherently good thermal stability [35].

The dynamic mechanical spectra of the hybrid films are shown in Fig. 10. T_g was taken from the temperature at

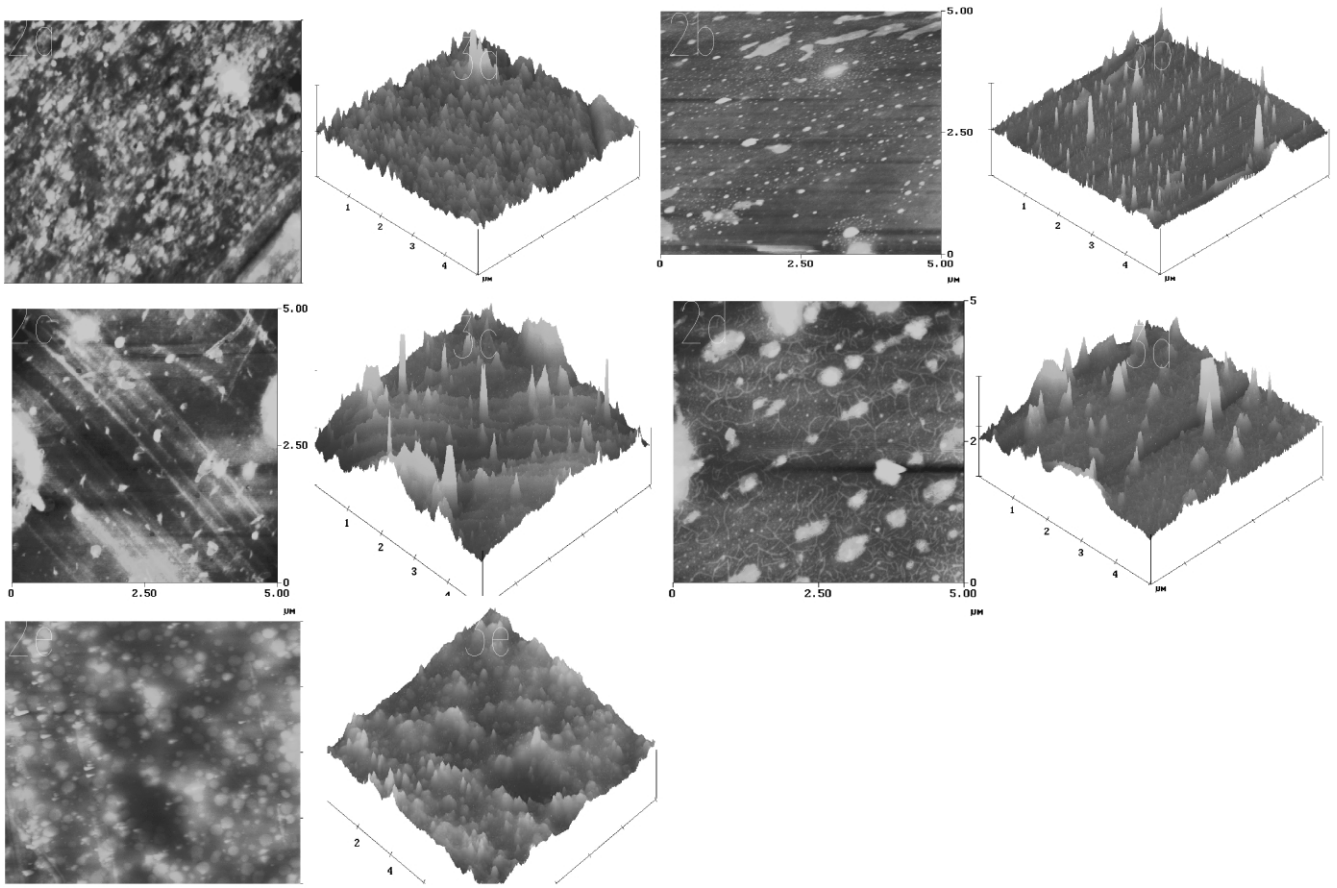

Fig. 6. Surface morphology of hybrid composite films.(2a, 3a): PI/TEVS5, (2b, 3b): PI/TEVS10, (2c, 3c): PI/TEVS20 (2d, 3d): PI/TEVS30, and (2e, 3e): PI/TEOS30, where 2 and 3 indicate the two- and three-dimensional images, respectively.

which the tan δ peak shows a maximum. The T_g of the hybrid composites increased with increasing the PVSSQ content. The improvement of the T_g comes from the strong interfacial interaction and possible covalent bonding between the polyimide and PVSSQ. The peak temperature of the tan δ curves, which corresponded to the T_g of the pure polyimide, shifted to higher temperature side with increasing the PVSSQ or TEOS content. The results suggest that the mobility of the polyimide chains was restricted by the interaction of the fairly dispersed PVSSQ or TEOS domains with the matrix polyimide, as well as the degree of cross-linking increased with increasing the amount of the PVSSQ.

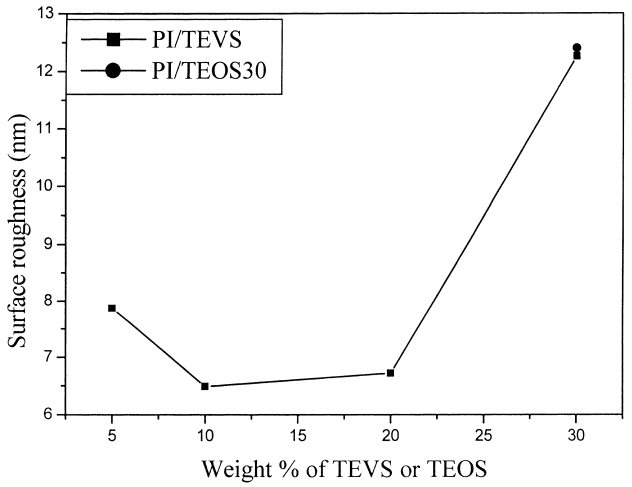

Fig. 7. Relationship between surface roughness and different weight% of TEVS (or TEOS30).

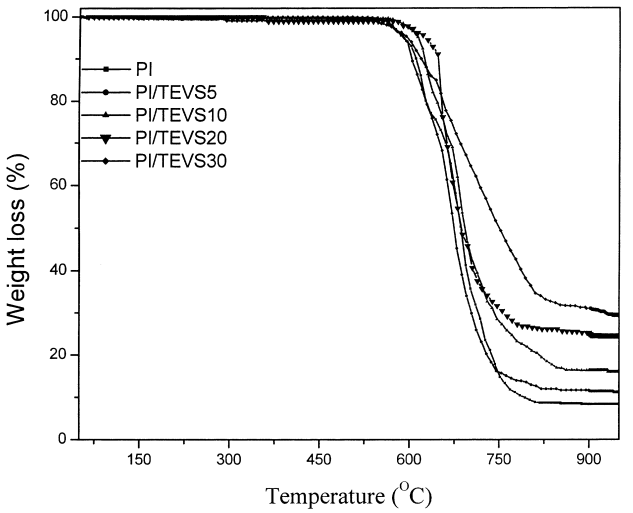

Fig. 8. Effect of TEVS contents on the thermal stability of hybrid films.

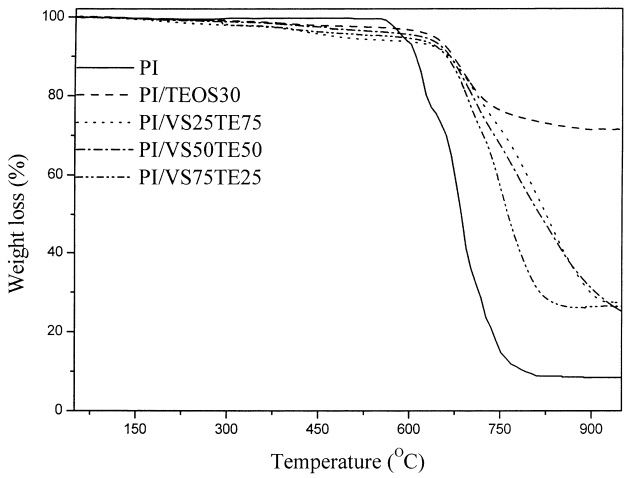

Fig. 9. Effect of the composition of TEOS and TEVS on the thermal stability of hybrid films.

The effects of TEOS contents on the tan δ behaviors, however, were not large. The observations showed in good agreement with the literatures [6,11,36].

3.5. Dielectric constant

The dielectric constant of the pure polyimide and polyimide/PVSSQ hybrid composite films with different PVSSQ contents are shown in Fig. 11. When small amounts of PVSSQ were introduced into PI, the dielectric constant was remarkably reduced but was found to be increased with further increasing PVSSQ content. However, the value of polyimide containing 30 wt% of PVSSQ is still lower than that of the pure polyimide. This phenomenon can be explained with the aid of the increasing free volume and domains sizes of PVSSQ. Higher PVSSQ content can cause the formation of bigger PSSQ domains, which is made of three-dimensional networks that bond PI block together and a bigger PVSSQ domains from higher amount of the PVSSQ contents may increase the separation between the PI interblock and increase in free volume. Usually, free volume

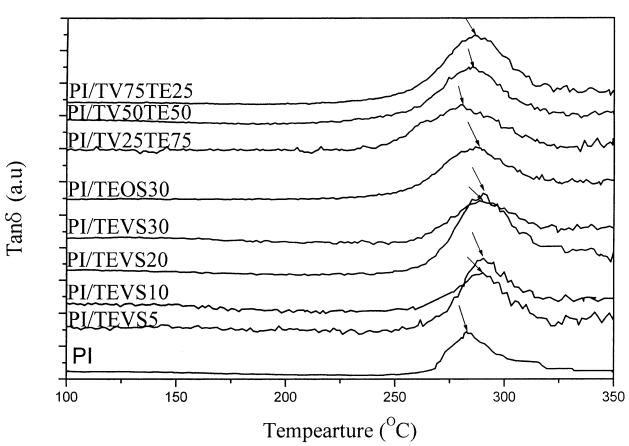

Fig. 10. Tan δ behaviors of pure polyimide, PI/TEVS and TEOS hybrid films.

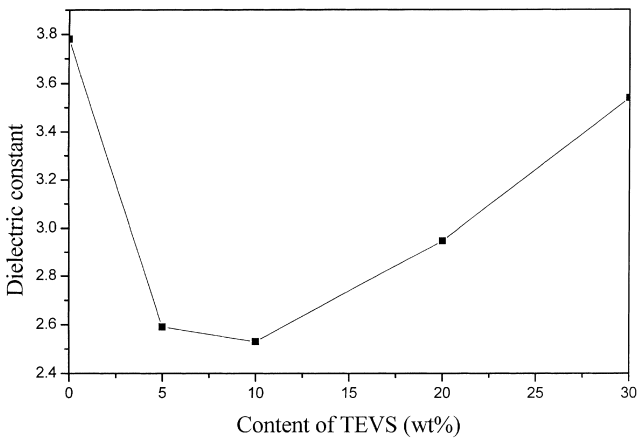

Fig. 11. Effect of TEVS contents on the dielectric constants of PI/TEVS hybrid films.

is easily occupied by moistures and increases the dielectric constant because of the inherently high dielectric constant, 80, of PVSSQ. However, PI/PVSSQ hybrid films are affected by the increase in free volume and probably the hydrophobicity of the PVSSQ domains. It may be assumed that the Si–O–Si and the Si–O bond in the cured network structures can also lead to increase the dielectric constant with increasing the content of the PVSSQ [24,26,37].

3.6. Mechanical properties

The tensile strength and elongation at break of the PI/PVSSQ hybrid films are plotted in Fig. 12. The simultaneous increase in tensile strength and elongation at break up to 10 wt% of PVSSQ contents result from the development of fine morphology in the hybrid films, which can obviously be attributed to a more efficient stress transfer mechanism between two components of hybrid composites. These phenomena might be distinctive features of nano-composites. When the PVSSQ content exceeds at $\geq$10 wt%, reduction in tensile strength can be found in Fig. 12, which is indicative of the larger domains of the

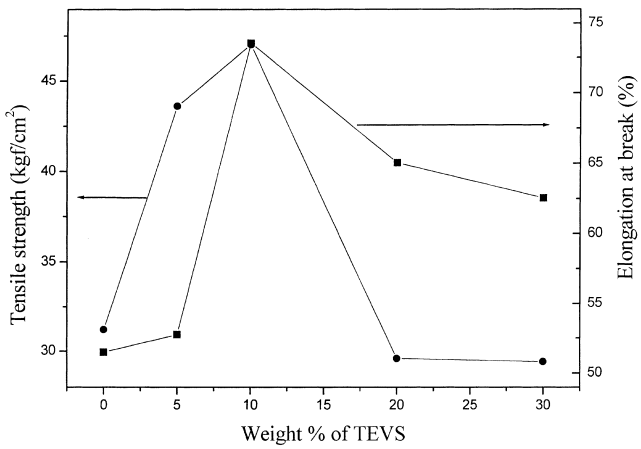

Fig. 12. Variation of mechanical properties of pure polyimide and hybrid composite films as a function of different weight% of TEVS.

PVSSQ due to the poor interfacial adhesion. It is noteworthy that the elongation at break decreased when the contents of PVSSQ is ≥20 wt% but the value is still higher compared to the pure PI matrix. The improvement of mechanical properties can be explained by the result of the introduction of fine silica particles into a polymer matrix and better adhesion as well as strong interaction between polyimide and the PVSSQ. This indicates that the flexible organic phase of PVSSQ plays a significant role in the interfacial adhesion between PI and the PVSSQ. As is well known, the strength should be reduced if there are no bonding sites between the organic polymer phase and the inorganic phase. The mechanical properties of the composites are generally dependent on the bonding between the two phases, the inorganic surface area of the filler, and the arrangement between the fillers. It is expected that if the PVSSQ might generate more organized composite films during the so called secondary condensation process at 200–250 °C, more improved mechanical properties would be obtained [38].

Fig. 13 shows the tensile strength and elongation at break of the PI/TEOS hybrid as well as the PI/TEOS/PVSSQ hybrids. The PI/TEVS30 hybrid showed higher mechanical properties compared to the PI/TEOS hybrid of the same TEOS contents. As the composition of TEVS relative to TEOS is increased in the hybrids, tensile strength and elongation at break are increased. The result is closely related to the finer morphology for the hybrid containing higher TEVS contents, as shown in Fig. 5. It is clear in Fig. 5 that small amount of loading such as TEOS25% in Fig. 5(h) produces better morphology, resulting in the improved mechanical properties. A similar explanation has already been reported in the literatures [6,17,39–41].

Before conclusion, the enhanced compatibility for the PI/PVSSQ hybrids in comparison to that of the PI/TEOS hybrids should be addressed again, with regard to the novelty of the present work. It has been well established that phase compatibilization between polyimide and silica can be achieved by chemical reaction between organsilane and polyimide matrix if one uses an organosilane as coupling

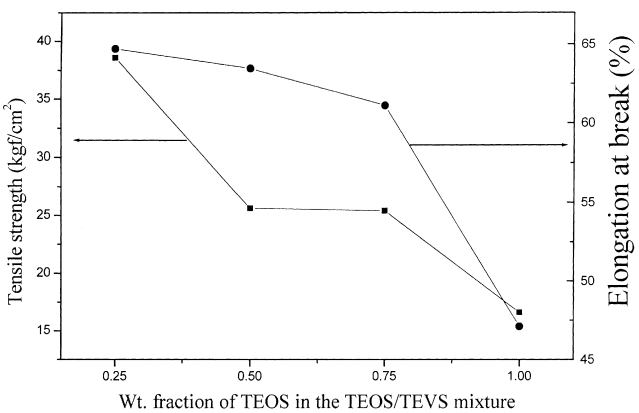

Fig. 13. Effect of composition of TEOS and TEVS on the mechanical properties of hybrid composite films containing different weight fraction of TEOS in the TEOS/TEVS mixture.

agent. The enhanced compatibility of the resultant hybrid composites using coupling agent may govern overall properties of final hybrid composites. In this work, it is believed that the organic part of PVSSQ plays a vital role to induce some chemical bonding as well as strong interaction such as hydrogen bonding between PVSSQ with PI matrix, as already suggested in SEM morphology in Fig. 5. This result should be noteworthy in that the enhancement of compatibility between PI and silica can be realized even when an organosilane coupling agent is not used for the system. From the systematic studies on the effect of PVSSQ on the morphology of the hybrid systems (in Fig. 5(e)–(h)) by using the mixtures of TEOS and TEVS, one can see clearly how the manner of these morphological changes according to the relative amounts of TEVS to TEOS affect on mechanical properties of the hybrid composites (Figs. 5, 12, and 13). We believe that this kind of systematic studies on the enhanced compatibility in the present work may give insight to the development of other novel hybrids of PSSQ derivatives and PIs for more versatile applications of the polyimide/silica based hybrid composites.

4. Conclusions

In this work, new hybrid composite films of polyimide and PVSSQ could be produced with the use of TEVS. The transparencies of the composite films were decreased with increasing the amount of the PVSSQ. The FTIR spectra confirmed the formation of Si–O–Si bond as well as the conversion of PAA into polyimide and hybrid composites films. The surface topography was influenced significantly by the compositions of PVSSQ. TGA results suggested that the thermal stability was improved with the increasing the amount of PVSSQ. Thermal stability and DMTA results suggested the stronger interaction as well as better interfacial interaction between the PI and PVSSQ rather than that between PI and TEOS. The dielectric constant of the hybrid composites ranged from 2.59 to 3.78. The interfacial interaction between the PI and PVSSQ has led to the improved mechanical properties of the hybrid composites. The fine dispersed morphology due to the interaction between two phases resulted in improved mechanical properties.

Acknowledgements

The work was supported by the National Research Laboratory Program, the Center for Integrated Molecular systems, POSTECH, Korea and the Brain Korea 21 Project.

References

[1] Special Issue on Organic–Inorganic Hybrid Nanocomposite Materials. Chem Mater 2001:(13):3059–3809.

[2] Mittal KL, editor. Polyimide; sythesis, characterization, and applications. New York: Plenum Press; 1983.
[3] Feger C, Khojasteh MM, McGrawth JE, Polyimide: materials, chemistry and characterization, Amsterdam: Elsevier; 1989.
[4] Gosh MK, Mittal KL. Polyimides, fundamentals and applications. New York: Marcel Dekker; 1996.
[5] Wilson D, Stenzenberger HD, Hergenrother PM, editors. Polyimide. Glassgow: Blackie; 1999.
[6] Mascia L, Kioul A. Polymer 1995;36:3649.
[7] Sroog CE. Prog Polym Sci 1991;16:561.
[8] Maier G. Prog Polym Sci 2001;26:3.
[9] Kransc B, Koops GH, Vander vegi NFA, Wesshing M, Wiibenhorst V, Turnhout JV. Adv Mater 2002;14:1041.
[10] Sharp KG. Adv Mater 1998;10:1243.
[11] Cornelius CJ, Marand E. Polymer 2002;43:2385.
[12] Jeng RJ, Chen YM, Jain AK, Kumer J, Tripathy SK. Chem Mater 1992;4:1141.
[13] Watanabe Y, Shibasaki Y, Ando A, Ueda M. Chem Mater 2002;14: 1762.
[14] Ellision M, Taylor LT. Chem Mater 1994;6:990.
[15] Nandi M, Colin JI, Salvati JL, Sen A. Chem Mater 1991;3:201.
[16] Morikawa A, Yamaguchi H, Kakimoto M, Imai Y. Chem Mater 1994; 6:913.
[17] Chen Y, Iroh JO. Chem Mater 1999;11:1218.
[18] Ha C-S, Park H-D, Frank CW. Chem Mater 2000;12:839.
[19] Kim Y, Ree M, Cho WJ, Chang T, Ha CS. Synth Met 1997;85:1399.
[20] Miller RD. Science 1999;286:421.
[21] Nguyen CV, Carter KR, Hawker CI, Hedrick JL, Jaffer RL, Miller RD, Remunar JF, Rhee HW, Rice PM, Toney MF, Trollsas M, Yoon DY. Chem Mater 1999;11:3080.
[22] Lichtenhan JD, Vu NQ, Carter JA, Gilma JW, Feher FJ. Macromolecules 1993;26:2141.
[23] Zhnag C, Laine RM. J Am Chem Soc 2000;122:6979.
[24] Tsai M, Whang W. Polymer 2001;42:4197.
[25] Hedrick JL, Cha HJ, Miller RD, Yoon DY, Brown HR, Srinivasan S, Pietro RD. Macromolecules 1997;30:8512.
[26] Homma T, Yamaguchi M, Kutsuzawa Y, Otsuka N. Thin Solid Films 1999;340:237.
[27] Xenopoulos C, Mascia L, Shaw SJ. J Mater Chem 2002;12:213.
[28] Sysel P, Hozova R, Sindelar V, Brus J. Polymer 2001;42:10079.
[29] Iyoku Y, Kakimato M, Imai Y. High Performance Polym 1994;6:53.
[30] Kim HI, Lee JK, Kim JB, Park ES, Park SJ, Yoo DY, Yoon DY. J Am Chem Soc 2001;123:12121.
[31] Becroft LL, Johnen NA, Ober CK. Polym Adv Technol 1997;73:289.
[32] Fately WG, Grasselli JG. The handbook of infrared and Raman characteristic frequencies of organic molecules. New York: Academic Press; 1991.
[33] Luo J, Lannutti JJ, Seghi RR. Mater Sci Engng C 1995;C5:15.
[34] Sharp KG. Adv Mater 1998;10:1243.
[35] Wen J, Wikes GL. Chem Mater 1996;8:1667.
[36] Hu Q, Marand E. Polymer 1999;40:4833.
[37] Lee HJ, Lin EK, Wang H, Wu WL, Chen W, Mayer ES. Chem Mater 2002;14:1845.
[38] Lee JK, Char K, Rhee HW, Ro HW, Yoo DY, Yoon DY. Polymer 2001;42:9085.
[39] Shang X, Zhu Z, Yin Y, Ma X. Chem Mater 2002;73:2977.
[40] Park HB, Kim JH, Kim JK, Leem YM. Macromol Rapid Commun 2002;23:544.
[41] Iyoku Y, Kakimato M, Imai Y. High Performance Polym 1994;6:95.